Journal of Applied Electrochemistry **29**: 511–520, 1999.

The feasibility of using a rechargeable MnO_2 cathode with a metal hydride anode

DEYANG QU
Emtech, Inc., 2486 Dunwin Dr., Mississauga, ONT, Canada L5L 1J9
(e-mail: qu@rayovac.com; present address: Rayovac Corporation, 601 Rayovac Dr., Madison, WI 53711, USA)

Received 9 February 1998; accepted in revised form 8 August 1998

Key words: bismuth, doping, manganese dioxide, metal hydride, rechargeable battery

Abstract

The feasibility of using a manganese dioxide cathode with a metal hydride anode is discussed. MnO_2 cathodes doped with bismuth compounds were rechargeable. The cathode material was prepared in its discharged state from MnO and bismuth compounds, thus matching the metal hydride anode in terms of initial state of charge, formation cycles and balance of self-discharge. It is believed that the presence of bismuth in the cathode prevents formation of spinel manganese oxide and lowers the activation energy (overpotential) for the second electron reduction and oxidation of MnO_2. Hydrogen recombination with MnO_2 was also studied to enable balancing of the self discharge rates of cathode and anode during storage.

1. Introduction

The search for clean and renewable power sources has been a major technological and environmental activity for several decades. Among the power sources being studied are primary and secondary battery systems. Some have been on the market and widely used for many years, including the alkaline MnO_2 battery, which is the most widely used type in daily life, the lead–acid battery employed in automotive applications and NiCd for aircraft and military uses as well as small rechargeable electronic devices and OEM applications. However, because of its toxicity and harmful effects to the environment, the NiCd battery is gradually losing its market share to the recently developed, but more expensive, Li-ion and nickel–metal hydride (Ni/MH) batteries, especially for high end OEM segments, and to the rechargeable MnO_2/ Zn battery successfully introduced to the market place by Rayovac under the brand name Renewal® for low end segments of OEM and consumer applications.

To develop a better MnO_2 material that can deliver its $2e^-$ capacity during discharge, attempts have been made to introduce dopant ions into manganese oxides using various methods [4]. A few dopant ions were tested but the real breakthrough occurred in 1977 by researchers from Hitachi [5] and in the early 1980s by Wroblowa and coworkers from the Ford Motor Company [6, 7] when the first truly rechargeable manganese dioxides were made. These chemically modified manganese dioxides were prepared by doping $MnO_2$with Bi or Pb ions. The resulting materials had no constraints connected with depth of discharge, as with EMD. The modified MnO_2 electrodes were not only fully rechargeable, but were insensitive to overdischarge and overcharge, unlike the majority of battery electrodes. They are also capable of high current drain [8].

In alkaline electrolytes, a high cell voltage can be achieved by coupling MnO_2 with Zn. However, Zn is highly soluble in alkaline solution. For the MnO_2/Zn system, it has been long known that migration of the zincate ion into the cathode during discharge is harmful to its performance, especially the rechargeability of manganese dioxide electrode [6, 7]. Formation of hetaerolite is assumed to be responsible. Therefore, replacing the soluble Zn anode with a solid state metal hydride or hydrogen anode may improve the cycle life of the battery [9–12]. The MnO_2 cathode material has certain advantages over the NiOOH material currently used in Ni/MH batteries, for example, lower cost, environmentally friendly and a low self discharge rate.

2. Experimental details

2.1. *Materials*

EMD was obtained from Kerr-McGee. MnO, Bi_2O_3 and Bi metal were purchased from Alfa. The metal hydride alloy was a IBA standard sample (IBA No1) with the formula $MmNi_{3.35}Co_{0.75}Mn_{0.4}Al_{0.3}$. KS-44 graphite was from Lonza. Chemically modified MnO_2 was prepared according to the Ford patent [13]. The Mn:Bi mole ratio was 20:1 for all Bi doped manganese oxide electrodes.

2.2. *Electrochemistry*

All electrochemical experiments were performed at 298 ± 1 K in 30% aqueous KOH electrolyte. All reported potentials are referred to a Hg/HgO reference electrode immersed in a KOH solution of the same concentration as the experimental electrolyte, unless otherwise noted. A Ni mesh was used as counter electrode. When an air tight cell was used, NiOOH/$Ni(OH)_2$ was used as the counter electrode to avoid gas generation. NiOOH/$Ni(OH)_2$ electrode was taken from a NiCd battery.

Manganese oxide compounds were mixed thoroughly with graphite at the desired ratio along with 0.5% (of dry material) of a Teflon suspension (DuPont T-60) as a binder in a high speed electric mixer for 10 min. The resulting active material (manganese oxide–Teflon-graphite) was rolled to form flexible films. Discs were punched out of the film and pressed onto a Ni current collector.

The metal hydride alloy (MH) was ground and screened. The particle size of used to make electrodes was $<45\,\mu$m. These electrodes were fabricated in the same manner as manganese oxide electrodes.

A flat cell capable of maintaining a high gas pressure was used in all the electrochemical tests.

2.3. *Hydrogen absorption*

A sealed cylindrical cell with an attached pressure transducer (OMEGA PX303-ASV) was used to investigate the reaction rate between MnO_2 and H_2. A hydrogen tank was connected to the cell. A pressed MnO_2 sample tablet was sealed in the cell and exposed to an H_2 environment. The pressure in the cell was adjusted with the hydrogen tank valve. Since the cell was not initially under vacuum, the partial pressure of hydrogen in the cell may vary. The cell was pressurised to 100 psi and the decrease in pressure was monitored over time with the pressure transducer. All pressures reported are the uncorrected values.

2.4. *Methods*

Constant current charge and discharge were carried out with an EG&G 173 potentiostat controlled by Q&R Smart Data Package. Data from the pressure transducer was also acquired using Q&R Smart Data.

3. Results and discussion

3.1. *Obstacles to combining a MnO_2 cathode with a metal–hydride anode*

3.1.1. *State of charge*

A battery must be constructed with the cathode and anode in the same state of charge. For instance, the active component of the alkaline Zn/MnO_2 cell cathode is $Mn^{IV}O_2$ and the anode is Zn^0. Each electrode is in its charged state and ready to be discharged. Alternatively, a Ni/MH cell is assembled with cathode in its reduced state ($Ni^{II}(OH)_2$) and the H_2 absorption metal alloy anode in the desorbed state. Therefore, this battery is made in its discharged state and must be charged before use.

If a MnO_2 cathode is combined with a H_2 absorption alloy anode in a cell, the state of charge of the two materials are mismatched. MnO_2 is in its charged state while metal hydride alloy is in its discharged state. Rather than the desired H_2 absorption/desorption reactions, discharging such a cell may result in oxidation of the alloy matrix to metal ions until the cell reaches 0 V. If instead the cell is charged, the MnO_2 cathode may oxidize to or MnO_4^{2-} or O_2 could evolve.

An MnO_2/MH cell requires the hydrogen absorption alloy in its charged state, but it is technically difficult to prepare ex situ metal hydride alloys containing absorbed hydrogen because they are not stable.

3.1.2. *Rate of self discharge*

In practical cells, the self discharge rate of the cathode and anode should be similar or be made similar. In a Li/MnO_2 cell the MnO_2 cathode is in its stable state and will not be self discharged. The Li anode tends to react with electrolyte solvents, but the reaction products form a passive layer on the Li surface preventing further reaction.

In a Zn/MnO_2 cell, like in a Li/MnO_2 cell, MnO_2 is stable. The Zn anode can react with aqueous KOH electrolyte solution to generate hydrogen gas unless it is amalgamated or alloyed with other metals, such as Pb, Bi or In, to increase the overpotential for hydrogen

evolution. Organic inhibitors may be added to the Zn anode to reduce the reaction between Zn and electrolyte if no Hg is present.

In the case of a Ni/MH battery, the state of charge and capacity decreases during storage due to self discharge. H atoms inside the metal alloy host lattice diffuse to the surface and recombine to form hydrogen gas. This process at the negative electrode is mainly responsible for the self discharge of Ni/MH batteries. The rate of the decomposition reaction increases with temperature. Fortunately, the positive electrode in its charged state (NiOOH) can react with the residual hydrogen to quantitatively form $Ni(OH)_2$. In this way, pressure build up can be avoided and the state of charge of both electrode can be balanced during storage.

However, in the case of MnO_2/MH cells, this mechanism to balance the hydrogen gas absorption alloy self discharge is absent. Even though the reaction between MnO_2 and H_2 is thermodynamically possible ($\Delta G < 0$), the reaction rate is extremely low and cannot match the rate of H_2 formation at the metal hydride anode. During storage, the cell pressure would increase, which could cause the cell to leak, and the states of charge of the cathode and anode would differ.

Accordingly, to use a rechargeable MnO_2 cathode with a metal hydride anode, not only the state of charge of MnO_2 and MH has to be made the same prior to cell assembly, but also the self discharge rate of both electrodes has to be balanced.

3.2. *Bi doped rechargeable MnO cathode*

Bi doped MnO_2 materials have been made by various processes [13–15] and have been shown to be rechargeable regardless of the synthetic method. In the simplest case, EMD can be transformed into a doped, rechargeable material by physically mixing it with Bi_2O_3. The resulting material is called 'physically modified' MnO_2 [16].

Bi doped MnO_2 can utilize its $2e^-$ capacity. The mechanism of the reduction and oxidation of Bi doped MnO_2 has been investigated in depth [17,18]. The final product of the electrochemical reduction was shown by X-ray absorption to be Mn^{II} (as $Mn(OH)_2$) with intergrowths of metallic Bi. The $Mn(OH)_2$ can be oxidized to MnO_2 in its original structure. The reduction and oxidation processes can be repeated many times [19, 20].

Based on this mechanism, it may be possible to make a rechargeable cathode for MnO_2/MH battery by mixing bismuth with Mn^{II} compounds. The cathode will be in its reduced (discharged) state. If it is rechargeable the problem with mismatched states of charge would be overcome.

Although the final product of MnO_2 reduction is $Mn(OH)_2$, the compound itself is unstable and is easily oxidized to MnOOH in moist air or lose water in dry air. However, MnO is a commercially available stable oxide, and was chosen as the starting material for the cathode. Figures 1(a) and (b) show the first nine charge and discharge curves, respectively, for the electrode made by physically doping MnO with Bi_2O_3. Figures 2(a) and (b) show the first nine charge and discharge curves, respectively, for physically doping MnO with metallic Bi powder. Since all the electrodes were initially in their discharged state, they were charged before the first discharge .

Three plateaux may be observed in both Figures 1(a) and 2(a). Figure 3 shows the second and third cycle of the cyclic voltammograms for Bi doped MnO_2 made by a chemical method. Three anodic peaks can be observed corresponding to each of three plateaus in Figures 1(a) and 2(a). The first plateau at −0.5 V Vs Hg/HgO may be associated with the oxidation of Bi to Bi_2O_3 while the other two plateaus at −0.25 V and 0.15 V may be associated with the two stage oxidation of Mn(II) involving the first and the second electron, respectively.

It is reasonable to assume from Figures 1(a) and 2(a) that some Mn(II) is oxidized at −0.5 V rather than Bi since the cathode in Figure 1(a) contains Bi_2O_3 and the capacity (in mAh) associated with plateau I in Figure 2(a) is greater than the capacity required to convert all of the Bi to Bi_2O_3. The plateaus I and II in Figures 1(a) and 2(a) represent about 40% of theoretical $2e^-$ capacity of MnO_2. It is not clear why the oxidation of Mn(II) to Mn(III) occurred in two potential ranges. However, EXAFS [19] showed that the Bi–O species are weakly associated with a Mn–O structure, thus there is the possibility of a recharge promotion or 'catalyst effect' by the Bi during the initial stages of charging that might arise from an adsorption effect at the surface of MnO_2 particles. Therefore, the Mn atoms which intimately contact Bi may be oxidized at a lower potential than that in the bulk of Mn–O particles.

The capacity associated with the plateau I at −0.5 V in Figure 1(a) was smaller than those in subsequent cycles. Besides contributing to the oxidation of some of the Mn(II) to Mn(III), it may be assumed that during the extensive mixing process, part of Bi_2O_3 reacted with MnO and became Bi metal.

In Figures 1(b) and 2(b), the capacity of the first discharge of the MnO_2 electrode doped with metallic Bi was higher than that of the electrode doped with Bi_2O_3. There was no −0.4 V plateau in the first discharge curve of the Bi_2O_3 doped MnO electrode (Figure 1(b)). This phenomenon may be explained by noting that Bi_2O_3 is more difficult to incorporate into the structure of MnO

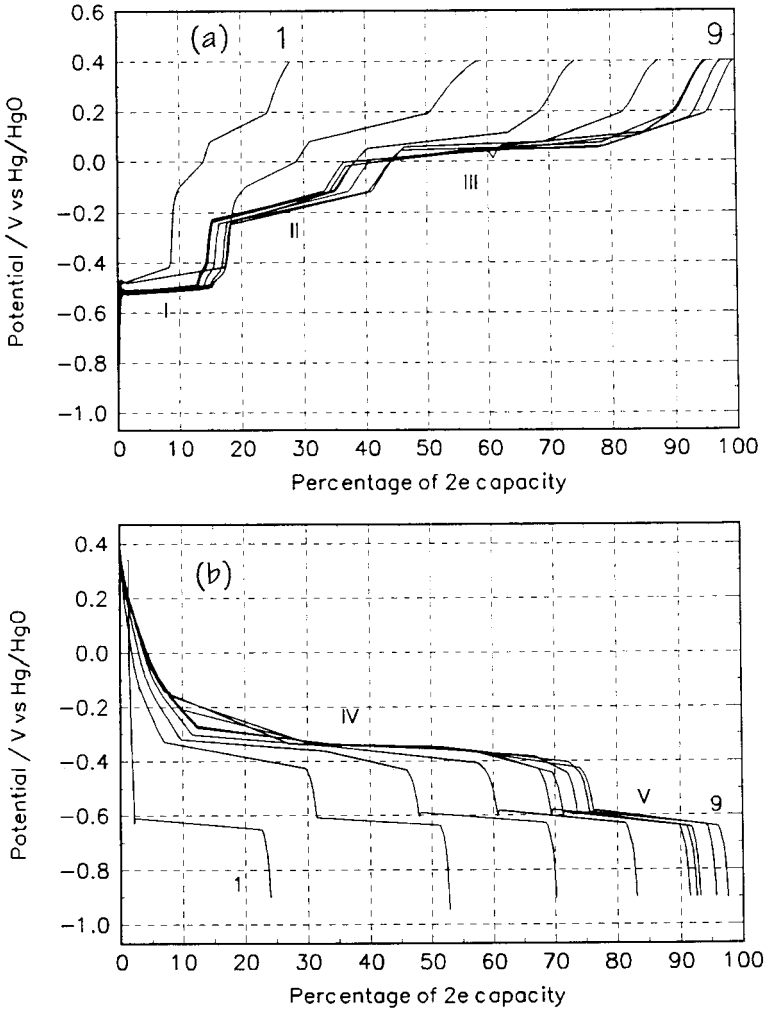

Fig. 1. Comparison of: (a) successive 1st to 9th constant current (0.16 A g^{-1}) charge curves with (b) discharge curves (at the same rate) at the MnO electrode physically mixed with Bi_2O_3 (molar ratio Mn:Bi = 20:1).

compared with metallic Bi. The second discharge in Figure 1(b) shows significant capacity at about the same voltage as the first discharge at MnO doped by Bi metal (in Figure 2(b)).

Interestingly, in Figures 1(a) and 2(a) the increase of the total capacity during cycling was mainly from the increase of the capacity associated with plateau III which, as mentioned previously, can be assumed to be associated with the process Mn(III) → Mn(IV). In both Figures 1(a) and 2(a), the capacity associated with plateau I and plateau II, which can be assumed to be associated with mixed Bi → Bi_2O_3 and Mn(II) → Mn(III) processes, did not change significantly during the first nine cycles (except the first charge). It is apparent that the oxidation of Mn(II) to Mn(III) can take place easily in the very early stage of the formation cycles and is less influenced by the existence of Bi dopant. However, the presence of Bi is critical for the oxidation process associated with Mn(III) → Mn(IV); the Mn(III) can only be fully converted to MnO_2 after a few formation cycles. At the same time Bi is incorporated into the structure. Therefore, in the Bi doped MnO electrode, the oxidation mechanism of Mn(II) to Mn(III) could be assumed to be similar with that of a γ-MnO_2 electrode, the intermediate product may be γ-Mn_2O_3 [21–23]. Bi could be considered to work as a 'catalyst' to reduce the activation energy needed to oxidize Mn(III) to Mn(IV), since the capacity gain occurs mainly in the plateau III charging process and there is little change in the first and second charging plateaus.

Figures 1(b) and 2(b) show the first nine discharge curves of a charged MnO cathode. Two plateaus can be distinguished at −0.4 V (plateau IV) and −0.6 V (pla-

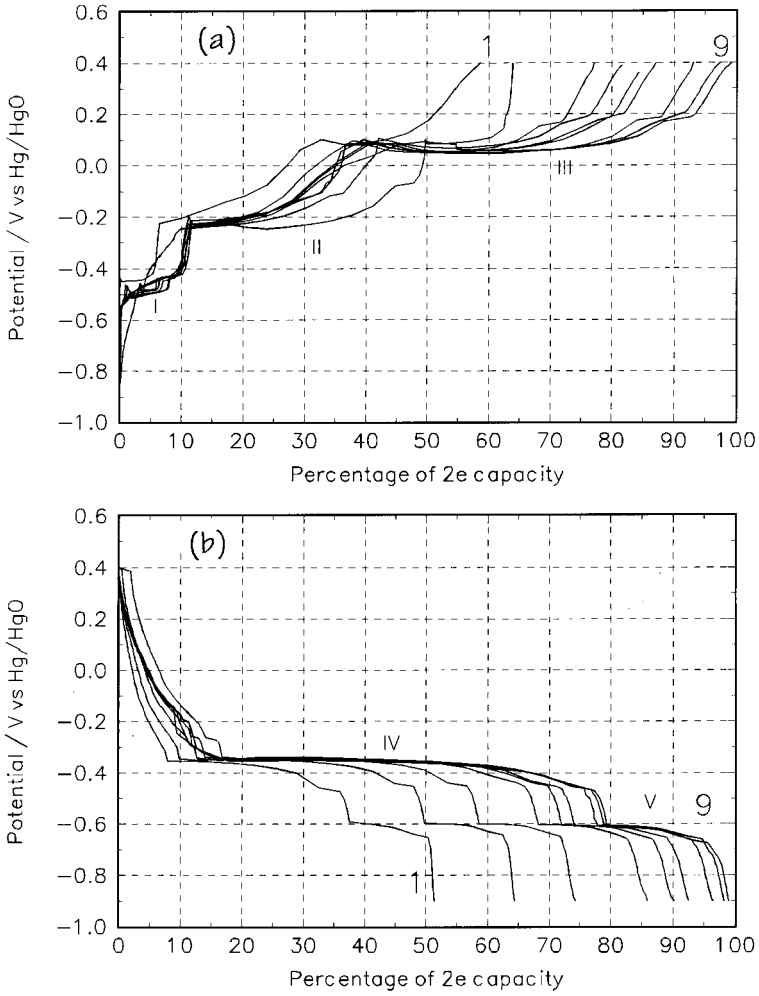

Fig. 2. Comparison of: (a) successive 1st to 9th constant current (0.16 A g^{-1}) charge curves with (b) discharge curves (at the same rate) at the MnO electrode physically mixed with Bi powder (molar ratio Mn:Bi = 20:1).

teau V), both voltages were measured against Hg/HgO. The majority of plateau V can be assumed to be the reduction of Bi_2O_3 to Bi, the capacity associated with plateau V is similar to plateau I. It is higher than the theoretical capacity of the $Bi_2O_3 \rightarrow$ Bi reduction, so it is reasonable to assume that part of the capacity at −0.6 V was a result of Mn(III) reduction to $Mn(OH)_2$. Plateau IV may be associated with the process $MnO_2 \rightarrow$ Mn(III) $\rightarrow$ $Mn(OH)_2$. Most of the MnO_2 has been shown to be reduced to $Mn(OH)_2$ at −0.4 V vs HgO/Hg [19].

On the one hand, in the reduction of γ-MnO_2, which is the intergrowth of ramsdellite and pyrolusite, protons are assumed to be inserted into the ramsdellite domains during the discharge of its first electron to form groutite which maintains its original lattice structure with an increase in lattice volume. This process is reversible. On the other hand, proton insertion into the rutile domains causes a transformation to a $Mn(OH)_2$ (pyrochroite) product which has a layered structure. Oxidation of layered $Mn(OH)_2$ forms Mn_2O_3 which can only be further oxidized to MnO_2 at very low rate [21]. It is believed that the structure incompatibility between groutite and pyrochroite limits the rechargeability of γ-MnO_2 electrodes in aqueous cells because of the energy required to transform between the two structures. Spinel Mn_3O_4 was found to be the intermediate product in the second and subsequent discharge steps if γ-MnO_2 was discharged to $Mn(OH)_2$ during first discharge [21, 22].

It is believed a heterogeneous mechanism including soluble Mn(III) species is the dominate process in the Bi doped MnO_2 electrode. Soluble Mn(III) species form at the early stage of the reduction induced by the presence

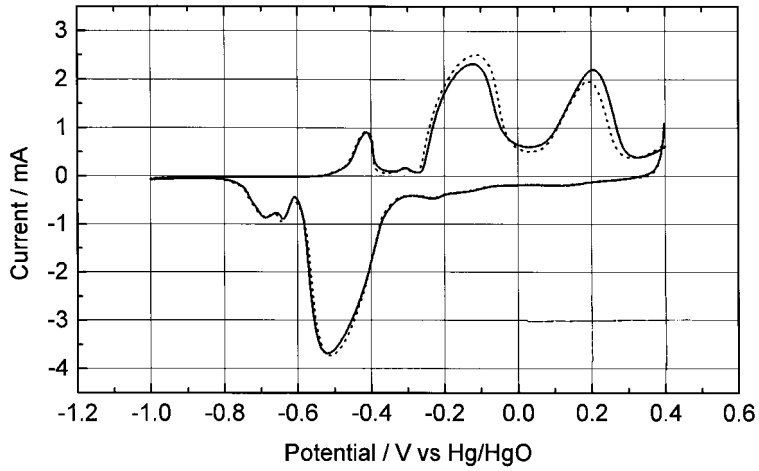

Fig. 3. The 2nd (——) and 3rd (- - - -) cycles of cyclic voltammetry for chemically modified MnO_2 (Mn:Bi molar ratio is 20:1), sweep rate: 0.5 mV s^{-1}.

of Bi. The formation of nonrechargeable spinel, which is the end product of the single phase homogeneous proton intercalation process, could be bypassed if the charge and discharge reactions proceed through the heterogeneous pathway. With the help of Bi, the reduction of Mn(III) to Mn(II) is much easier compared to that of γ-MnO_2 in which Mn(III) can only be reduced at more negative potential and much lower rate. Considering the catalytic impact of Bi in the oxidation of Mn(III) to MnO_2, it is reasonable to assume that the main effect of Bi doping is to reduce the activation energy (overpotential) of the charge and discharge processes involving Mn(III).

3.3. *Formation cycles*

For most types of secondary batteries (except Renewal), before shipping from the plant, they must be cycled under controlled charge–discharge procedures. The role of the formation cycles is to activate the cell since the full capacity of the cells may not be achieved at the first and second discharge. Figure 4 shows the first nine charge and discharge curves for IBA No. 1 metal hydride alloy. The full capacity of the material was not delivered until after five charge–discharge cycles. This activation procedure can cause process engineering problems because of gas generation during the formation cycles due to unbalanced anode and cathode capacities.

There is general agreement that activation processes are surface related. The surface 'as-fabricated' may not be suitable for electrochemical operation in the electrolyte and needs to be modified in situ. For example, a solid electrolyte interface (SEI) is formed on the surface

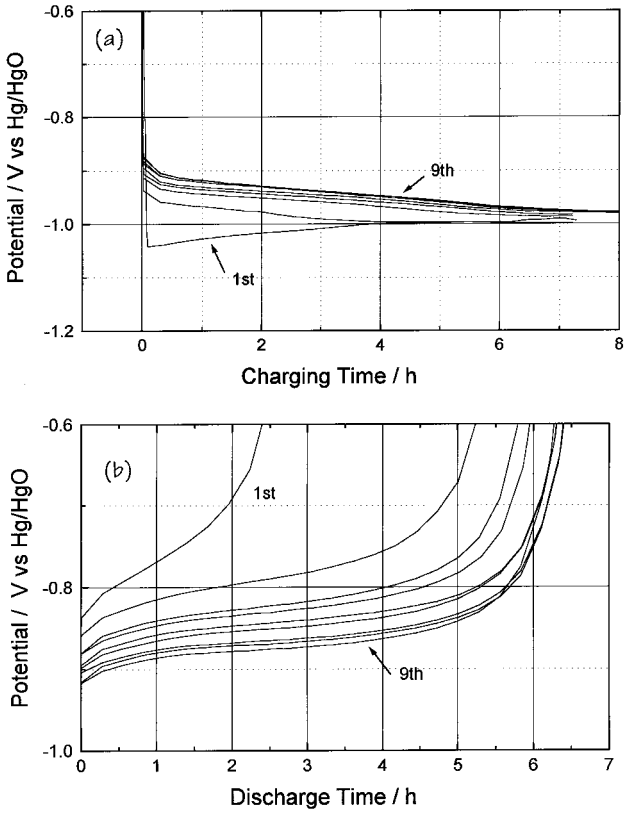

Fig. 4. Comparison of: (a) successive 1st to 9th constant current (0.045 A g^{-1}) charge curves with (b) discharge curves (at the same rate) at the IBA No. 1 metal hydride electrode.

of a carbon anode that prevents further reaction between the electrode and electrolyte during the formation cycles of Li-ion cells. In the case of a metal hydride anode, it is believed that the alloy has an oxidized

surface layer, the oxide layer is not a good electronic conductor, but has a very important role in the hydrogen absorption/desorption reactions by providing catalytic sites, protecting the metal hydride from oxidation and preventing H_2 diffusion from the bulk of the electrode to the surface region. It is also generally agreed that hydrogen goes through an adsorbed intermediate and that the hydrogen coverage and catalysis of to the H—H bond breakage are important parameters defining the kinetics of the entry of hydrogen into the metal. Figure 4(a) shows that not only *IR* drop at the beginning of charge decreased during the first nine cycles, but also the overpotential of hydrogen insertion decreased. This indicates the conductivity of the electrode increased and the kinetics of hydrogen insertion improved during the formation process.

Due to the difficulties associated with in situ electrochemical formation in the cell fabrication processes, ex situ chemical activation processes have been investigated (e.g., etch treatments). However, the difficulty of electrochemical formation could be solved by using Bi-doped MnO as the cathode with a metal hydride anode. Figure 5 shows the comparison of the formation cycles for the IBA No.1 metal hydride anode and the MnO cathodes doped with Bi_2O_3 and Bi. As mentioned previously, both types of electrodes need to be formed by initial charge and discharge cycles after the electrodes are fabricated. The increased capacities during the formation cycles are similar for the metal hydride anode and the Bi doped MnO cathodes. The maximum capacity of both types of electrodes can be reached within five to six cycles. Therefore, if a MnO cathode and a metal hydride anode are balanced, it should be possible for the capacity of the cathode and the anode to be matched during the course of formation cycles, thus gas generation could be minimized or even eliminated.

3.4. *Hydrogen recombination with manganese dioxide cathode*

During MnO/MH cell storage, hydrogen will evolve due to the self-discharge of metal–hydride anode, as mentioned in Section 3.1.2. As the consequence, not only can excessive gas pressure build up in an sealed cell, but the state of charge between the manganese oxide cathode and metal hydride anode will differ. The MnO_2 cathode in general does not have the capability of recombining hydrogen and the evolved gas is usually vented, causing water loss or increased internal pressure in sealed cells. Depending on the amount of hydrogen present and the rate of gas generation, excessive pressure can cause rupture of the safety vent resulting in cell failure and electrolyte leakage.

To address the problem, manganese dioxide must be made to react with H_2. MnO_2 has little ability to absorb hydrogen gas, but MnO_2 can chemically react with hydrogen in the presence of catalysts. Kozawa and Kordesch [24, 25] reported that palladium and silver oxide can be excellent catalysts for the MnO_2–H_2 reaction. Figure 6 shows the hydrogen absorption rate at MnO_2 electrodes containing various percentage of Ag_2O catalyst. MnO_2 alone shows little reaction with

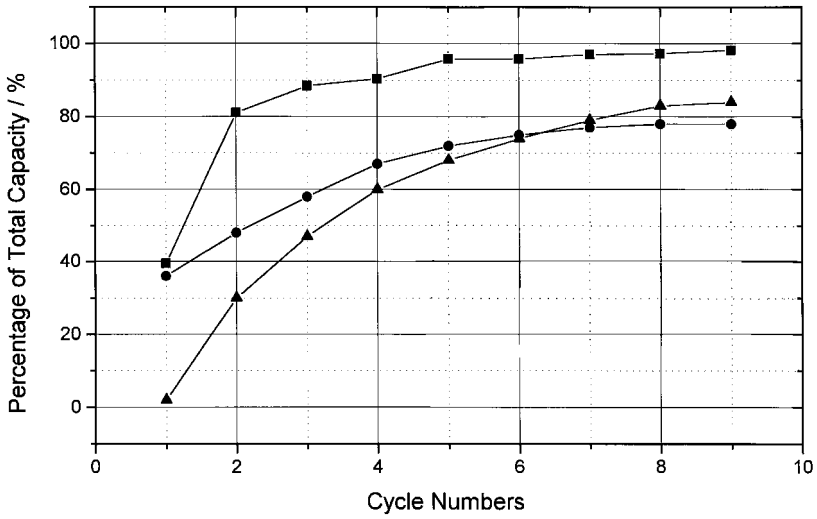

Fig. 5. Comparison of the capacity increase during formation cycles of the IBA No1 metal–hydride (■), Bi_2O_3 doped MnO (▲) and Bi doped MnO (●) electrodes.

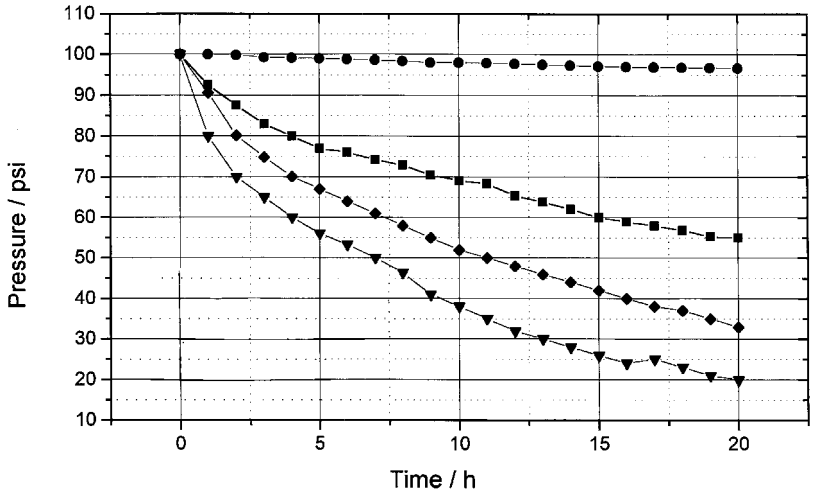

Fig. 6. Comparison of hydrogen absorption rate at MnO_2 electrodes with various percentages of Ag_2O: (●) 0% , (■) 1% , (◆) 3% and (▼) 4%.

H_2, the slight decrease of hydrogen pressure could due to the leakage of the cell rather than consumption by reaction with MnO_2. The hydrogen absorption rate depends on the percentage of Ag_2O. The higher the percentage of catalyst the faster the absorption rate.

The absorption rate was faster initially and subsequently slowed. This can be explained by understanding the reaction mechanism between H_2 and MnO_2. The redox reaction between MnO_2 and H_2 takes place at the solid–gas interface of the electrode first, then protons diffuse into the bulk of the electrode, while electrons move in the opposite direction to the surface of electrode. At the initial stage of the reaction, the rate of the reaction is determined by the surface area of the interface between the solid phase of manganese dioxide and the gaseous phase of hydrogen, as the reaction proceeds, the rate of absorption gradually becomes determined by the diffusion rate of proton/electron within the solid phase of manganese dioxide, which is believed to be a slow process.

A significant decrease in the absorption rate was observed if the electrode was exposed to 30% KOH electrolyte. This may be explained if the MnO_2 particles were covered with electrolyte and hydrogen had to diffuse through the film to reach the MnO_2 particles. The diffusion rate, however, becomes the rate determining step.

The rate of the self discharge of the metal hydride anode increases with temperature, thus the rate of hydrogen generation increases as well. Fortunately, as

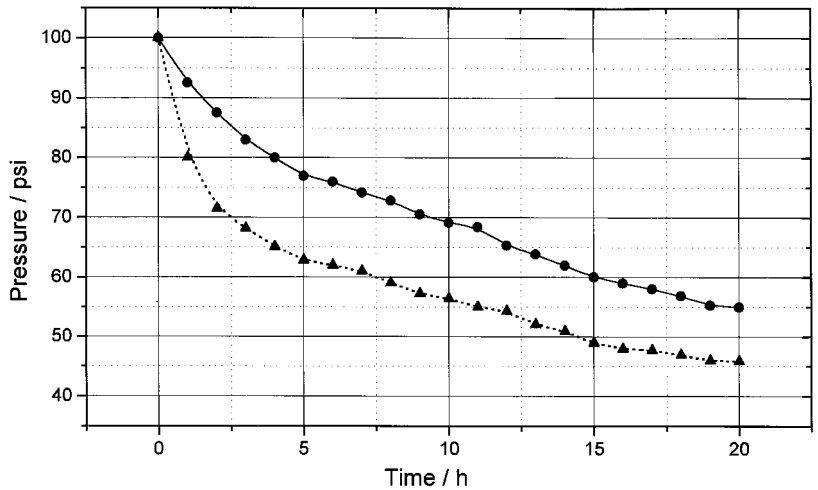

Fig. 7. Comparison of hydrogen absorption rate at MnO_2 electrode mixed with 1% of Ag_2O at 273 K and 318 K. Key: (●) 298 K and (▲) 318 K.

show in Figure 7, the hydrogen absorption rate at MnO_2 electrodes also increases with temperature so the excess hydrogen generated at high temperature can be absorbed.

It should be emphasized that the choice of hydrogen absorption catalyst is determined by the cathode/anode ratio, because the products formed during the reduction of MnO_2 by H_2 depend on the catalyst [26]. If silver oxide is used, MnO_2 will be reduced to MnOOH and sometimes slightly lower than Mn(III). If Pd is used, the product is Mn(II). Obviously, the hydrogen absorption capacity of Pd catalyzed manganese dioxide is about twice that of silver oxide catalysed manganese dioxide. Therefore, if the cell is designed to be anode limited, Ag_2O is a good candidate because of its lower cost, but if cathode limitation is required, than Pd should be considered instead.

3.5. *Bi-doped MnO/metal–hydride cell*

As discussed in the previous Sections, a MnO/metal–hydride cell can be theoretically assembled. However, even overcoming the two major obstacles mentioned in Sections 3.1.1 and 3.1.2, much engineering work must be done to construct a practical cell with these two electrodes. Necessary process developments include fabrication of the cathode and the anode, selection of a proper metal hydride alloy to match the formation cycles of MnO cathode, balancing the capacity of the two electrodes and electrolyte balance, among others. Although cell development is not within the scope of this paper, Figure 8 shows the first five cycles of a cell containing excess electrolyte made with a Bi metal doped MnO cathode and a IBA No. 1 metal–hydride anode. A nonwoven separator was used. The experiment was conducted in an open cell (the flat cell with valve opened) so the small amount of gas generated in each cycle would not accumulate in the cell. The gas generation resulted from the unbalanced cathode and anode during the formation cycles. The cell was made based on 70% of $2e^-$ capacity of the MnO_2 cathode and 80% of maximum attainable capacity of IBA No. 1 alloy.

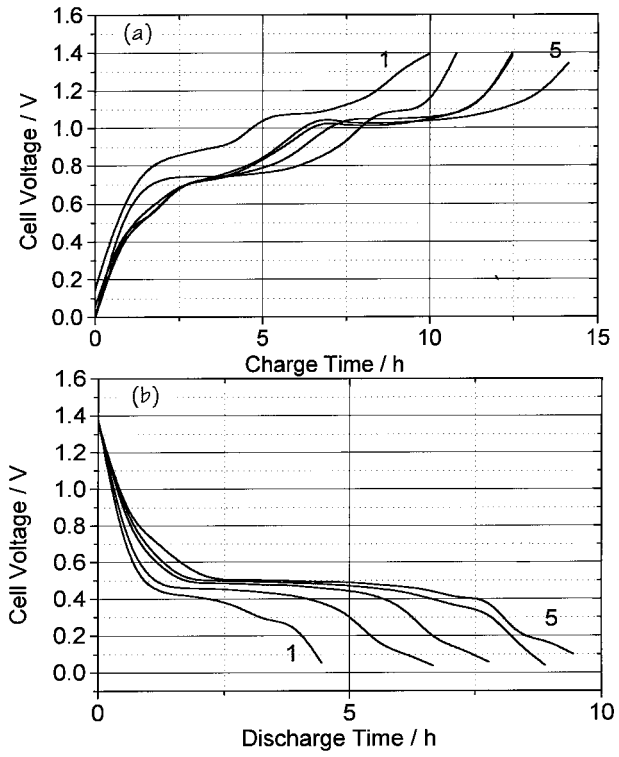

Fig. 8. Comparison of: (a) first five constant current (150 mA) charge curves with (b) discharge curves (at the same rate) for MnO/metal–hydride (IBA No. 1) lab cell.

As shown in Figure 8(a) and (b), after a few cycles of formation, the capacity of the MnO/MH cell is stabilized. As constructed, the cell was in its discharged stage, like $Ni(OH)_2$/MH cells. It was charged before being discharged and the full capacity was achieved after a few cycles. It should be noted that the plateau voltages in the discharge curves are at about 0.5 V. Although the cell voltage could be marginally increased by choosing a better metal hydride alloy and adopting an optimized method of electrode fabrication, the low voltage is intrinsic to the MnO/MH system as determined by the thermodynamics of the MnO_2 and metal hydride electrodes. The low cell voltage may impede its use in single cell designs, but it could have advantages in multicell battery modules like those used in electric vehicle applications.

4. Conclusions

(i) It is theoretically possible to make a cell with a manganese oxide cathode and metal hydride anode. The fundamental obstacles of electrode capacity and self discharge balances can be overcome by using Bi doped MnO to ensure the same state of charge for both electrodes prior to cell assembly and using Ag_2O or Pd catalyst to balance the self discharge during storage.

(ii) The roles of Bi in the manganese oxide electrode are to avoid the formation of a nonrechargeable spinel phase and to reduce the activation energy of the second electron oxidation/reduction step.

(iii) A MnO/MH cell would operate below 1 V, which could restrict its application as a single cell, but it could possibly be used in battery packs or in a bipolar configuration.

Acknowledgements

Grateful acknowledgment is made to Dr B.E. Conway and researchers in his group for useful and stimulating discussions. The author is indebted to his colleague in Rayovac Corporation, Dr M.J. Root, for reviewing the manuscript.

References

1. K. Kordesch, J. Gsellmann, M. Peri, K. Tomantschger and R. Chemelli, *J. Electrochimica Acta* **26** (1981) 1495.
2. D. Guyomard and J.M. Tarascon, *J. Electrochem. Soc.* **139** (1991) 937.
3. L. Li and G. Pistoia, *Solid State Ionics* **47** (1991) 231.
4. Niroki Tamura, Kenji Ishizeki, Mosaichi Nagayama and Ryusaburo Furuichi, *J. Electrochem. Soc.* **141** (1994) 2035.
5. JA 0041846
6. Y.F. Yao, N. Gupta and H.S. Wroblowa, *J. Electroanal. Chem.* **223** (1987) 107.
7. M.A. Dzieciuch, N. Gupta and H.S. Wroblowa, *J. Electrochem. Soc.* **135** (1988) 2415.
8. L. Bai, D.Y. Qu, B.E. Conway, Y.H. Zhou, G. Chowdury and W.A. Adams, *J. Electrochem. Soc.* **140** (1993) 884.
9. D.Y. Qu, PhD Thesis, University of Ottawa, Canada (1994).
10. A.J. Appleby, H.P. Dhar, Y.J. Kim and O.J. Murphy, *J. Power Source* **29** (1990) 333.
11. K. Kordesch, L. binder, J. Gsellmann, E. Kahraman and G. Winkler, *J. Power Sources* **13** (1991) 273.
12. X. Xia and Z. Guo, *J. Electrochem. Soc.* **144** (1997) L213.
13. Y.F. Yao, *US Patent 4 520 005* (1985).
14. R.C. Kainthia and D. J. Manko, *US Patent 5 156 934*.
15. C. Zhang, *US Patent 5 250 374*.
16. H.S. Wroblowa and N. Gupta, *J. Electroanal. Chem.* **238** (1987) 93.
17. D.Y. Qu, B.E. Conway, L. Bai, Y.H. Zhou and W.A. Adams, *J. Appl. Electrochem.* **23** (1993) 693.
18. D.Y. Qu, L. Bai and B.E. Conway, *J. Electroanal. Chem.* **365** (1994) 247.
19. B.E. Conway, D.Y. Qu and J. McBreen, *in* 'Synchrotron Techniques in Interfacial Electrochemistry', (edited by C.A. Melendre and A. Tajeddine Kluwer Academic, Amsterdam, (1994), pp. 311–344.
20. B.E. Conway, D.Y. Qu, L. Bai, W.A. Adams, G. Choudhary and J. McBreen, *in* Proceedings of the Symposium on the Science of Advanced Batteries, edited by D. Scherson, The Ernest B. Yeager Centre for Electrochemical Science, Case Western Reserve University, Cleveland, OH (1995).
21. J. McBreen, *J. Power Sources* **5** (1975) 525.
22. L.T. Yu, *J. Electrochem. Soc.* **144** (1997) 802.
23. M. Bode, Co Cacbet, S. Bach, J.P. Pereira-Ramos, J.C. Ginous and L.T. Yu, *J. Electrochem. Soc.* **144** (1997) 792.
24. A. Kozawa and R.A. Powers, *Electrochem. Tech.* **5** (1967) 535.
25. A. Kozawa, *J. Electrochem. Soc.* **123** (1976) 1193.
26. A. Kozawa and K. Kordesch, *Electrochim. Acta* **26** (1981) 1493.